The Open Agriculture Journal
DOI: 10.2174/0118743315460508260408080804, 2026, 20, e18743315460508
ISSN: 1874-3315
1

RESEARCH ARTICLE **OPEN ACCESS**

Identification, Characterization, and Expression Analysis of the IMPβ Nuclear Transport Protein Gene Family in *Taraxacum kok-saghyz*

Qing-yu Yang[1,†], Wei Ma[1,†] and Xue-yan Zhang[1,*]

Ministry of Education Key Laboratory for Ecology of Tropical Islands, College of Life Sciences, Hainan Normal University, Haikou, China

Abstract:

Introduction: *Taraxacum kok-saghyz* (*TKS*), a perennial member of the Compositae family, is one of the three most important rubber-producing plants globally, alongside *Hevea brasiliensis* and *Parthenium hysterophorus*. Natural rubber is a vital industrial raw material with significant economic and daily-life implications. The *importin β* (*IMPβ*) gene family in *H. brasiliensis* has been implicated in the transport of ethylene-induced proteins associated with rubber biosynthesis. However, the role of the *IMPβ* gene family in *TKS* remains unexplored.

Methods: In this study, we identified 27 *TKS importin β* (*TkIMPβ*) gene family members. These members contain conserved domains and were classified into 12 subfamilies using multiple sequence alignment, phylogenetic analysis, and protein motif characterization.

Results: Bioinformatics analysis revealed replication-based relationships among four groups of TkIMPβ members: *TkIMPβ1/TkIMPβ2*, *TkIMPβ9/TkIMPβ14*, *TkIMPβ17/TkIMPβ18*, and *TkIMPβ22/TkIMPβ23*. Expression analysis indicated that certain *TkIMPβ* genes are associated with rubber biosynthesis, suggesting their regulatory role in natural rubber production.

Discussion: Subcellular localization and yeast two-hybrid assays (Y2H) confirmed that TkIMPβ proteins function as nuclear transport proteins rather than transcription factors, facilitating nuclear material transport and signal transduction. Additionally, exposure to NaCl stress, methyl jasmonate (MeJA), and ethylene (Eth) further demonstrated the involvement of *TkIMPβ* genes in rubber biosynthesis and stress responses.

Conclusion: Therefore, these findings not only improve our understanding of the evolution and expression patterns of the IMPβ family in *TKS* but also identify potential gene targets for molecular breeding strategies to enhance rubber yield in *TKS*.

Keywords: *Taraxacum kok-saghyz*, Rubber-producing plants, Importinβ (IMPβ) gene family, Natural rubber biosynthesis.

*Address correspondence to this author at the Ministry of Education Key Laboratory for Ecology of Tropical Islands, College of Life Sciences, Hainan Normal University, Haikou, China; Tel: 18568898899;
E-mail: zhangxueyan_caas@126.com
† These authors contributed equally to this work.

Cite as: Yang Q, Ma W, Zhang X. Identification, Characterization, and Expression Analysis of the IMPβ Nuclear Transport Protein Gene Family in *Taraxacum kok-saghyz*. Open Agric J, 2026; 20: e18743315460508.
http://dx.doi.org/10.2174/0118743315460508260408080804

Received: November 18, 2025
Revised: December 23, 2026
Accepted: January 12, 2026
Published: July 23, 2026

1. INTRODUCTION

Natural rubber (NR), or cis-1,4-polyisoprene, is an essential raw material in various industries, distinguished from synthetic rubber by its unique chemical properties [1]. *Hevea brasiliensis*, native to the Amazon rainforest, is currently the only natural rubber crop cultivated on a large scale. However, its high production costs and long cultivation cycles contribute to significant environmental impacts on tropical rainforests [2]. *Taraxacum kok-saghyz* (*TKS*), commonly known as Russian dandelion, is a perennial herb of the Compositae family [3]. Originating from inland Kazakhstan, the Junggar Basin, and the

Tarim–Tex River Basin in Xinjiang, China, it is now widely distributed across the Northeast Plain, North China Plain, and Northwest China [3, 4]. *TKS* is ranked among the world's top three rubber-producing plants, along with *H. brasiliensis* and *Parthenium hysterophorus*. Its roots contain a hydrocarbon polymer that is structurally and functionally similar to the NR polymer found in the latex tubes of *H. brasiliensis* [5]. The short growth cycle, ease of cultivation, and relatively simple genetic transformation make it an ideal model for studying plant-based rubber production. Since its discovery in the 1930s, researchers in China, the United States, and the Soviet Union have investigated its rubber content, chemical properties, agronomic requirements, and morphology. However, following the end of the Cold War and shifts in the global political landscape, major natural rubber producers in Southeast Asia and South America re-entered the market, leading to an oversupply of NR and a decline in *TKS* research [4-7].

Since the 21st century, the global automotive industry has expanded considerably, driving a sharp increase in NR demand. However, rubber trees thrive only in specific tropical climates, resulting in severe NR shortages in many countries. China, for instance, imports about 80% of its supply [8]. To mitigate these shortages, identifying alternative rubber-producing plants that can grow outside tropical regions is crucial. Since 2000, interest in TKS has been renewed among Chinese researchers. Unlike *H. brasiliensis*, *TKS* offers comparable rubber production along with several advantages, including a sevenfold faster production rate, a highly mechanized cultivation process, adaptability to temperate zones, and tolerance to poor soil fertility. Therefore, *TKS* is considered a promising alternative source of NR.

The primary distinction between eukaryotic and prokaryotic cells is that eukaryotic cells possess a nucleus enclosed by a double membrane [9]. The nucleus serves as the central hub for genetic material storage, replication, transmission, selective expression, and cellular metabolism [10]. The exchange of materials and information between the nucleus and cytoplasm is crucial for regulating cellular activities [11]. The nuclear transport system consists of two main components: nuclear transport receptors and nuclear pore proteins, whose interaction facilitates nuclear transport [12]. While small molecules diffuse passively across the nuclear envelope, macromolecules such as proteins require active transport mediated by nuclear transport receptors [12, 13]. Nucleocytoplasmic transport is a highly dynamic process involving the assembly, translocation, and disassembly of the import complex in a continuous cycle. Proteins such as importins, exportins, nucleoporins (Nups), and the cellular apoptosis susceptibility (CAS) protein participate in this process [14, 15], each playing distinct roles to ensure efficient transport [16]. Most biomacromolecules with molecular weights exceeding 50 kDa areactively transported by karyopherins [17-19]. Nuclear transport receptors, primarily belonging to the RanGTP-binding protein family, include importin α (IMPα) and importinβ (IMPβ), which share a conserved structural framework. IMPα acts as an adaptor, linking cargo proteins at one end while interacting with IMPβ or its homologs at the other. In plants, the function of IMPβ proteins extends far beyond basic nucleocytoplasmic shuttling. Studies have shown that IMPβ, as a core member of nuclear transport receptors, precisely regulates plant growth, development, environmental adaptation, and immune responses by specifically recognizing and transporting key transcription factors involved in various hormone signaling pathways and stress responses [20, 21]. For example, in *Arabidopsis*, the Importin β protein SAD2 has been shown to play a crucial role in stomatal immunity and abscisic acid (ABA) signal transduction by mediating the nuclear import of the protein phosphatase ABI1 [22]. In potato, an IMPβ gene induced by salicylic acid and hydrogen peroxide has been proven to be essential for plant responses to abiotic stress [21].

The pathways and regulatory mechanisms governing rubber biosynthesis pose significant theoretical challenges [1]. NR synthesis involves membrane proteins embedded in rubber particles within rubber-producing plants. These plants store and biosynthesize NR in their lactiferous ducts, with small rubber particles in laticifer cells serving as key organelles for both processes [1]. Unlike the nuclear-cytoplasmic transport of macromolecules, small molecular hormones regulate cellular signaling by binding to hormone receptors located either inside or outside the nucleus. This interaction modulates cell proliferation and immune responses. Extensive studies have explored the nuclear-cytoplasmic transport of hormone-receptor protein complexes, which initially assemble in the cytoplasm. Using yeast-based screening, Li et al. identified the AtJAT1 transporter as a key component in jasmonic acid (JA) transport. Functional analysis in *Arabidopsis thaliana* revealed that AtJAT1 mediates the nuclear import of extracellular JA and JA-Ile, significantly enhancing JA metabolism, particularly the cytoplasm interactions of JA-Ile [23]. However, the mechanism by which AtJAT1 facilitates JA-Ile transport across the nuclear double membrane remains unclear.

IMPβ binds to nuclear pore complex (NPC) proteins and plays a crucial role in nuclear protein transport. Based on the direction of cargo movement, IMPβ nuclear transport proteins are classified as exportins (mediating nuclear export) and importins (mediating nuclear import) [17-19]. At least 16 IMPβ subfamily members have been identified in eukaryotes, where the entire IMPβ family is expressed. In plants such as *Zea*, the IMPβ gene family exhibits significant expansion, with as many as 27 members identified, suggesting broad functional diversification [20].

This study presents the first comprehensive genome-wide analysis and characterization of the IMPβ nuclear transport protein gene family in *TKS*, using publicly available genome and transcriptome data. Bioinformatics analysis revealed replication-based relationships among four groups of IMPβ gene members: *TkIMPβ1*/*TkIMPβ2*,

TkIMPβ9/*TkIMPβ14*, *TkIMPβ17*/*TkIMPβ18*, and *TkIMPβ22*/*TkIMPβ23*. Phylogenetic analysis classified 27 IMPβs into 12 subfamilies. Expression analysis further showed that *TkIMPβ3* and *TkIMPβ16* exhibited the highest expression levels in *TKS* roots. Moreover, IMPβs in *TKS* appear to play multiple roles in natural rubber biosynthesis.

2. MATERIALS AND METHODS

2.1. Identification of IMPβ Gene Family Members in TKS

The genomic data for *TKS* (BioProject: PRJNA792143) were retrieved from the National Center for Biotechnology Information (NCBI). Protein sequences of the IMPβ gene family members from *Arabidopsis thaliana* and *Oryza sativa* served as query sequences, and candidate *IMPβ* genes in *TKS* (e-value < 1e-5) were identified through local BlastP analysis. The conserved domains of IMPβ, including the N-terminal Ran-binding domain, intermediate HEAT repeat domain, and C-terminal substrate / adapter-binding domain, were predicted using InterProScan (http://www.ebi.ac.uk/interpro). To improve confidence, these predictions were cross-validated with the Pfam. All candidate sequences were manually inspected; those lacking complete open reading frames or exhibiting fragmented domain architectures were discarded. Finally, 27 non-redundant *TkIMPβ* gene family members were identified. The isoelectric point and molecular weight of the corresponding proteins were predicted using the "Calculate" tool in the Expasy online database of the Swiss Center for Protein Bioinformatics (http://web.expasy.org/compute_pi/) [24].

2.2. Chromosome Localization and Replication Analysis

MapInspect software was used to analyze the chromosomal distribution of IMPβ genes based on genome annotation data. DAMAN software was used to compare the genetic relationships among the 27 IMPβ genes, with nucleic acid sequences showing >90% homology defined as duplicated genes [25]. Subcellular localization was predicted using the WoLF-PSORT online server [26].

2.3. Motif Analysis

The MEME online software was used to analyze amino acid sequences and identify conserved motifs in IMPβ proteins [27].

2.4. Phylogenetic Tree Construction and Exon-intron Structure Analysis

The Clustal W program in the molecular evolution analysis software MEGA6.0 was used to compare IMPβ protein sequences from *TKS*, *Arabidopsis thaliana*, *Hevea brasiliensis*, and *Oryza sativa*. The neighbor-joining (NJ) method with a bootstrap test of 1000 replicates was used to construct phylogenetic trees, which were then evaluated [28]. Gene structure analysis was performed using the online tool GSDS by comparing the coding DNA sequences (CDS) of rubber grass IMPβ genes with their corresponding genomic sequences [29].

2.5. Distribution of Cis-acting Elements in Promoter Regions

To study cis-acting elements in the promoter region of *IMPβ* genes in *TKS*, sequences 2000 bp upstream of each IMPβ initiation codon were retrieved from the *TKS* genome database. These sequences were analyzed using the online tool PlantCARE to predict cis-acting elements [30].

2.6. Gene-specific Expression Analysis

IMPβ gene expression levels were analyzed using RNA-sequencing data from different tissues and developmental stages of *TKS*; the raw sequencing data analyzed in this study were sourced from the NCBI BioProject database (accession: PRJNA539838) [31]. Briefly, clean reads were obtained after filtering raw data to remove low-quality sequences and were aligned to the *TKS* reference genome using HISAT2. Gene expression levels were normalized using the FPKM (Fragments Per Kilobase of transcript per Million mapped reads) method. Differential expression between samples was statistically assessed with the DESeq2 package, where genes with $|\log_2(\text{fold change})| \geq 1$ and an adjusted p-value<0.05 were considered significant. For visualization, the FPKM values were log-transformed as ln (X+1) and subsequently used to generate a heatmap. The final heatmap of IMPβ expression was created using Multi-Experiment Viewer (MeV) software [32].

2.7. Subcellular Localization

The coding sequences of *TkIMPβ10*, *TkIMPβ11*, and *TkIMPβ27*, excluding the stop codons, were independently cloned into the pCAMBIA Super 1300-GFP vector at the *Hind* III and *Kpn* I restriction sites to construct 35S::GFP-*TkIMPβ10*, 35S::GFP-*TkIMPβ11* and 35S::GFP-*TkIMPβ27*. The primer sequences for these constructs were designed using Primer Premier 5 (Table **1**). For transient expression analysis, *Nicotiana benthamiana* leaves were infiltrated with *Agrobacterium tumefaciens* (GV3101) carrying 35S::GFP-*TkIMPβ10*, 35S::GFP-*TkIMPβ11*, 35S::GFP-*TkIMPβ27*, or a control vector. The infiltrated plants were grown for three days, stained with DAPI, and observed under an LSM710 microscope (Zeiss, Germany) to detect green fluorescent protein (GFP) fluorescence signals.

2.8 Transcriptional Activation Assay

The corresponding vectors were also transformed into yeast strains. The full-length sequences of *TkIMPβ10*, *TkIMPβ11*, and *TkIMPβ27* (primers listed in Table **1**) were cloned into the *EcoR* I and *Sal* I sites of the pGBKT7 vector (TaKaRa, Nanjing, China, Cat. No. 630489). Synthetic plasmids expressing each protein were then transformed into yeast. The interaction between pGBKT7-53 and pGADT7-T (TaKaRa, Cat. No. 630442) served as a positive control. Transcriptional activation was analyzed as described previously [33]. Transformed cells were cultured on SD/-Trp and SD/-Trp/-His/-Ade plates, and recombinant colonies were visualized after 3–5 days of incubation at 30 °C.

Table 1. Primers for *TkIMPβ10*, *TkIMPβ11*, and *TkIMPβ27* gene experiments. Underline indicates the enzyme cutting site.

Primer Name	Sequence(5' to 3')	For experiment
GFP-*TkIMPβ10* F	ATCGACTCTAGAAAGCTTCAACCAAAGGAAGAAGGCCTG	Subcellular Localization
GFP-*TkIMPβ10* R	CTTGCTCACCATGGTACCCAATAGGCAGCGTTCCCATGA	
GFP-*TkIMPβ11* F	ATCGACTCTAGAAAGCTTGCGTAAACATGCAGAAGAAAG	
GFP-*TkIMPβ11* R	CTTGCTCACCATGGTACCAGAAATTGCACGACTTATGGC	
GFP-*TkIMPβ27* F	ATCGACTCTAGAAAGCTTATGGACGATTCAACTCAGCAA	
GFP-*TkIMPβ27* R	CTTGCTCACCATGGTACCCACAACATTTAGTCTCGAAAG	
Y2H-*TkIMPβ10* F	GCCATGGAGGCCGAATTCCAACCAAAGGAAGAAGGCCTG	Transcriptional Activation Assay
Y2H-*TkIMPβ10* R	CGGCCGCTGCAGGTCGACCAATAGGCAGCGTTCCCATGA	
Y2H-*TkIMPβ11* F	GCCATGGAGGCCGAATTCGCGTAAACATGCAGAAGAAAG	
Y2H-*TkIMPβ11* R	CGGCCGCTGCAGGTCGACAGAAATTGCACGACTTATGGC	
Y2H-*TkIMPβ27* F	GCCATGGAGGCCGAATTCATGGACGATTCAACTCAGCAA	
Y2H-*TkIMPβ27* R	CGGCCGCTGCAGGTCGACCACAACATTTAGTCTCGAAAG	
q-*TkIMPβ10* F	CTAAACTCCCACATCAATC	RTq-PCR
q-*TkIMPβ10* R	ATACTCATCCCACTAACAA	
q-*TkIMPβ11* F	CTTAAAACAGTTCCAGGAGCA	
q-*TkIMPβ11* R	TCTATGTTGTTCCTTGGCATC	
q-*TkIMPβ27* F	GTAGCTCATCGGATCGGGATA	
q-*TkIMPβ27* R	CTCTGTACCTGCCAACTCGAT	
GADPH F	AGTTGGTTTCGTGGTATGAC	
GADPHR	ACATGTCAGTGAACAGGTAGAC	

2.9. Plants Sowing and Treatments

The experiment was conducted in 2021–2022 using well-grown, uniformly sized, sterile *TKS* seedlings 20 days after sowing. The selected plants underwent the following treatments:

2.10. Nacl Stress Treatment

The plants were removed from the medium, and their roots were thoroughly washed with tap water to eliminate any residual medium. They were then quickly immersed in a solution containing 200 mM NaCl. Root samples were collected at 6, 12, and 24 h after treatment to analyze gene expression responses to salt stress. Three biological replicates were conducted at each time point. The control group was treated with distilled water containing 2.2% anhydrous ethanol.

2.11. Methyl Jasmonate and Ethylene Spraying Treatment

For hormone treatments, *TKS* leaves were sprayed with either 100 mg/L ethylene (Eth) or 0.8 mM methyl jasmonate (MeJA). Plants treated with distilled water containing 2.2% anhydrous ethanol served as controls. Root samples were collected at 6, 12, and 24 h after treatment to assess gene expression responses to hormones. Each treatment included three replicates.

2.12. Rtq-pcr of Impβ Gene after Nacl and Hormone Treatment

After treatment, root samples, including those from control plants, were collected at 6, 12, and 24 h. To ensure result reliability and reproducibility, samples for each treatment condition were collected from three different individuals to analyze gene responses to salt stress and hormone application (primers used are listed in Table **1**). GAPDH (Genebank: DY821911) was selected as the reference gene for normalization in this study. It has been previously validated as a stable reference gene in *TKS* roots under various abiotic stress and hormone treatment conditions [34]. The SYBR Green qRT-PCR reaction mixture contained 5 µl of 2× SYBR Green PCR buffer, 0.5 µl of primers, and 5 ng of template DNA, with the total volume adjusted to 10 µl using double-distilled H_2O. The PCR program comprised an initial step at 50 °C for 2 min, followed by 10 min at 95 °C, then 40 cycles of 95 °C for 15 s and 60 °C for 1 min. Data were analyzed using the $2^{-\Delta\Delta Ct}$ method [35].

2.13. Data Analysis

Microsoft Excel 2010 (Microsoft Corporation, Redmond, WA, USA) was used to organize raw data and calculate the mean and standard deviation for the control and each treatment. Figures were also generated using Microsoft Excel 2010. Statistical significance was set at $p < 0.05$.

3. RESULTS

3.1. Identification of IMPβ Family Members of TKS

IMPβ gene family members from model organisms such as *Arabidopsis thaliana* and Oryza sativa were retrieved from NCBI and used to identify *IMPβ* gene family members in *TKS* through local BLAST analysis. The BLASTP program identified 43 *TkIMPβ* candidate genes (e-value < 1e-5). Pfam analysis was then conducted to confirm the presence of the protein kinase domain and the

conserved *IMPβ* active center sequence, leading to the identification of 27 *TkIMPβ* gene family members. These genes were distributed across 26 distinct scaffold fragments within the assembled genome. Gene names were assigned based on scaffold size and chromosomal position, resulting in designations from *TkIMPβ1* to *TkIMPβ27* (Fig. **1**). The open reading frames (ORFs) of *TkIMPβ* genes in *TKS* varied in length, with *TkIMPβ12* being the shortest (276 bp) and *TkIMPβ27* the longest (3531 bp). The encoded proteins ranged from 91 to 1176 aa in length, with relative molecular masses between 10.38 kD and 130.22 kD. *TkIMPβ24* had the lowest isoelectric point (4.60), while *TkIMPβ11* had the highest (6.26). Chromosome location analysis revealed that *TkIMPB1*, *TkIMPB5*, *TkIMPB8*, *TkIMPB10*, *TkIMPB13*, *TkIMPB18*, *TkIMPB22*, *TkIMPB23*, *TkIMPB24*, and *TkIMPB26* were located in the cytoplasm. Furthermore, *TkIMPB3* and *TkIMPB20* were located in both the cytoplasm and nucleus, while *TkIMPB15* and *TkIMPB21* were present in both the cytoplasm and mitochondria. TkIMPβ14 was located in the vacuole, whereas the remaining gene family members were localized in the nucleus (Table **2**).

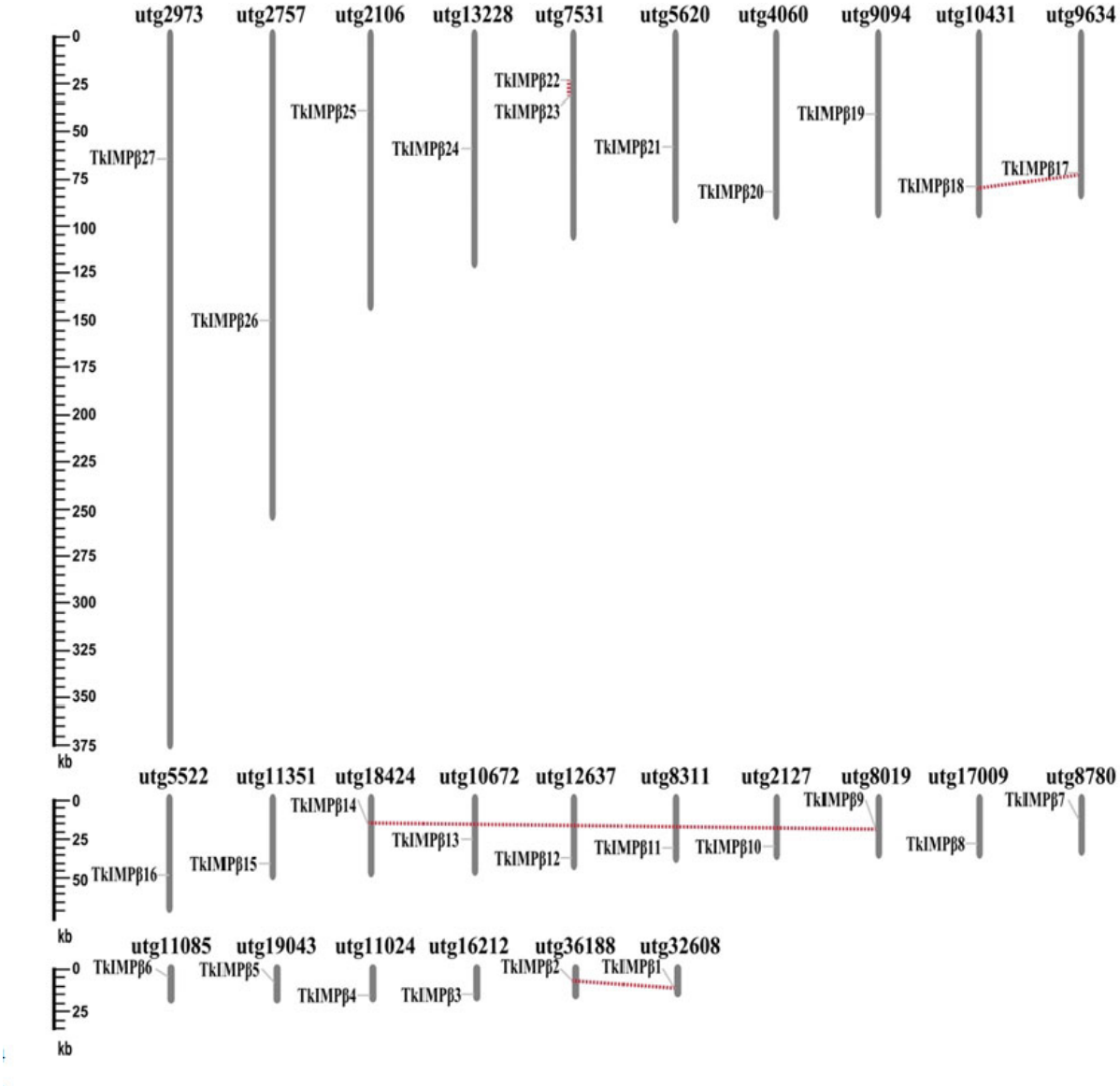

Fig. (1). Location of *IMPβ* genes on chromosomes in *TKS*. Twenty-seven *TkIMPβ* genes were located on 26 different genomic scaffolds. The naming order of *IMPβ* members was based on the scaffold length, and four groups of replicators were indicated by a red dotted line (nucleic acid homology > 90%). The scale on the left represents the chromosome length (kb), the Utg number at the top represents the chromosome name, and the solid line on the scaffold of 26 genomes indicates the position of the corresponding gene on the chromosome.

Table 2. Information regarding the *IMPβ* gene family in *TKS*.

Gene	Gene ID	ORF/bp	Protein			
			Size/aa	(MW/kD)	pI	Subcellular Localization
TkIMPB1	evm. TU. utg32608.5	3024	1007	112.33	4.84	Cytoplasmic
TkIMPB2	evm. TU. utg36188.3	3126	1041	116.07	4.87	Nuclear
TkIMPB3	evm. TU. utg16212.6	2913	970	108.78	5.42	Cytoplasmic, Nuclear
TkIMPB4	evm. TU. utg11024.4	1623	540	61.43	5.92	Nuclear
TkIMPB5	evm. TU. utg19043.5	3369	1122	123.71	4.82	Cytoplasmic
TkIMPB6	evm. TU. utg11085.1	2970	989	113.63	5.53	Nuclear
TkIMPB7	evm. TU. utg8780.5	2610	869	97.00	4.98	Nuclear
TkIMPB8	evm. TU. utg17009.9	3216	1071	123.23	5.44	Cytoplasmic
TkIMPB9	evm. TU. utg8019.8	3096	1031	113.94	4.76	Nuclear
TkIMPB10	evm. TU. utg2127.5	2892	963	107.01	5.33	Cytoplasmic
TkIMPB11	evm.TU. utg8311.5	3162	1053	119.11	6.26	Nuclear
TkIMPB12	evm. TU. utg12637.8	276	91	10.38	5.26	Nuclear
TkIMPB13	evm. TU. utg10672.2	3186	1061	122.08	5.94	Cytoplasmic
TkIMPB14	evm. TU. utg18424.4	3096	1031	113.97	4.78	Vacuolar
TkIMPB15	evm. TU. utg11351.9	3375	1124	125.00	5.96	Mitochondrial, Cytoplasmic
TkIMPB16	evm. TU. utg5522.8	3342	1113	123.15	4.76	Nuclear
TkIMPB17	evm. TU. utg9634.17	3336	1111	122.89	4.72	Nuclear
TkIMPB18	evm. TU. utg10431.21	3207	1068	118.20	4.71	Cytoplasmic
TkIMPB19	evm. TU. utg9094.7	3219	1072	119.89	5.55	Nuclear
TkIMPB20	evm. TU. utg4060.12	2667	888	98.07	4.63	Cytoplasmic, Nuclear
TkIMPB21	evm.TU. utg5620.9	2703	900	101.95	5.98	Mitochondrial, Cytoplasmic
TkIMPB22	evm. TU. utg7531.4	3078	1025	117.39	4.85	Cytoplasmic
TkIMPB23	evm.TU. utg7531.5	3081	1026	117.53	4.91	Cytoplasmic
TkIMPB24	evm. TU. utg13228.6	2619	872	96.93	4.60	Cytoplasmic
TkIMPB25	evm. TU. utg2106.11	3162	1053	115.29	4.82	Nuclear
TkIMPB26	evm. TU. utg2757.32	2592	863	96.03	4.68	Cytoplasmic
TkIMPB27	evm. TU. utg2973.12	3531	1176	130.22	5.62	Nuclear

3.2. Analysis of Conserved Motif Distribution of IMPβ Gene Family Members in TKS

Motifs 3, 5, 9, 10, 11, 12, 17, 18, 19, 20, 21, 22, 23, 24, 25, 26, 29, 30, 31, 32, 33, 34, 35, 36, 37, and 38 were found in the IBN-N domain. Motifs 2, 6, 7, 8, 9, 13, 14, 15, 27, 31, and 37 were present in the HEAT domain. Motifs 33 and 38 were identified in the Cse1 domain, while Motif 37 was found in the CAS-Cse1 domain. Motifs 1, 20, 34, 37, 38, 39, and 40 were associated with the Xpo1 domain.

Additionally, motifs 4, 16, and 28 were present in the CRM1-C domain.

To investigate the evolutionary conservation of *IMPβ* sequences in *TKS*, we analyzed the distribution of conserved motifs across 27 *IMPβ* gene family members using MEME. A total of 40 conserved motifs were predicted. Phylogenetic analysis revealed that members with close genetic relationships exhibited similar conserved motif distributions (Fig. **2**).

The number of motifs in each *TkIMPβ* ranged from 0 to 9. Identical motif patterns were observed in *TkIMPβ1* and *TkIMPβ2*; *TkIMPβ3* and *TkIMPβ4*; *TkIMPβ16*, *TkIMPβ17*, and *TkIMPβ18*; *TkIMPβ22* and *TkIMPβ23*; *TkIMPβ24* and *TkIMPβ26*; *TkIMPβ8* and *TkIMPβ13*; and *TkIMPβ9* and *TkIMPβ14*. Some motifs were unique to specific genes: Motif 31 to *TkIMPβ7*, Motif 36 to *TkIMPβ11*, Motif 39 to *TkIMPβ6*, and Motif 40 to *TkIMPβ10*. Additionally, Motifs 1, 3, 4, 16, 25, and 28 were unique to *TkIMPβ8* and *TkIMPβ13*; Motifs 5, 10, 12, 29, and 38 were unique to *TkIMPβ22* and *TkIMPβ23*; Motifs 17, 18, and 22 were unique to *TkIMPβ9* and *TkIMPβ14*; and Motifs 15, 26, and 32 were unique to *TkIMPβ2*.

The motif distribution patterns described above elucidate the functional and structural basis of the *TKS* IMPβ family. The conserved motifs enriched in domains such as HEAT and IBN-N constitute HEAT repeat units composed of α-helical pairs. The superhelical skeleton assembled from these units serves as the core structural basis for the interaction of IMPβ proteins with the nuclear pore complex (NPC), RanGTPase, and cargo proteins [36, 37]. Furthermore, the compositional differences in motifs between importins (*e.g.*, those containing the IBN-N domain) and exportins (*e.g.*, those containing the Xpo1 or CRM1-C domains) directly determine the specificity of their nucleocytoplasmic transport direction. It is noteworthy that some member-specific motifs (*e.g.*, Motif 31 in *TkIMPβ7*) are likely located in the variable loop regions responsible for substrate recognition [38]. This structural diversity enables different *TkIMPβ* members to precisely transport specific “cargoes,” including hormone and stress-response factors, thereby underpinning their broad functional diversity in *TKS*.

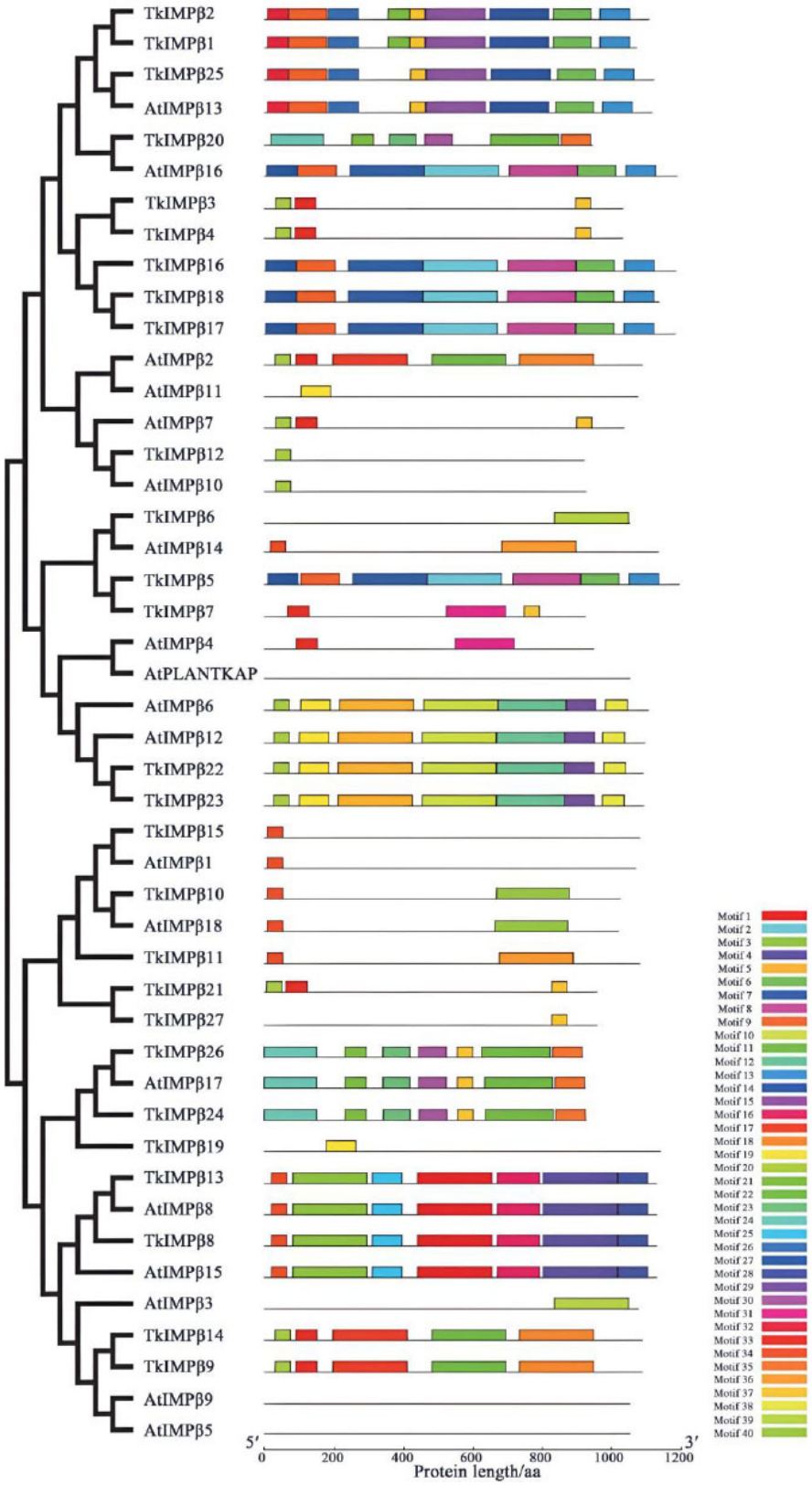

Fig. (2). Conserved motifs in IMPβ proteins were identified using the MEME online software based on amino acid sequence analysis.

3.3. Evolution Analysis of the IMPβ Gene Family in TKS

To better understand the evolutionary relationship between the *IMPβ* gene families of *TKS* and various species, we constructed a phylogenetic tree including *Arabidopsis thaliana* (19 IMPβs), *Hevea brasiliensis* (29 IMPβs), *Oryza sativa* (8 IMPβs), and *TKS* (27 IMPβs) (Fig. **3**).

Based on the phylogenetic tree structure, *IMPβs* were classified into 12 subfamilies. *TkIMPβ16*, *TkIMPβ17*, and *TkIMPβ18* clustered in subgroup D; *TkIMPβ10*, *TkIMPβ11*, and *TkIMPβ27* in subgroup E; *TkIMPβ5*, *TkIMPβ6*, *TkIMPβ7*, *TkIMPβ9*, *TkIMPβ14*, and *TkIMPβ21* in subgroup F; *TkIMPβ22* and *TkIMPβ23* in subgroup G; *TkIMPβ20* in subgroup H; *TkIMPβ12* in subgroup I; *TkIMPβ3*, *TkIMPβ4*, *TkIMPβ8*, *TkIMPβ13*, and *TkIMPβ25* in subgroup K; and *TkIMPβ19*, *TkIMPβ24*, and *TkIMPβ26* in subgroup G. Subgroups A, B, and C contained no *TKS IMPβ* genes, possibly due to functional differentiation over long-term evolution. Analysis of conserved domains within these 12 TkIMPβ subfamilies revealed that subgroup D members exclusively possessed the HEAT domain. While *TkIMPβ11*, resembling *HbIMPβ29* in the rubber tree, contained only the IBN-N domain, other subgroup E members exhibited either the IBN-N and Xpo1 domains or only the Xpo1 domain. In group J, *TkIMPβ15* possessed only the Xpo1 domain, whereas other members contained either the IBN-N, Cse1, and CAS-Cse1 domains or the IBN-N, Xpo1, and CRM1-C domains.

Group K members contained both the IBN-N and HEAT domains, whereas the remaining subgroup members possessed only the IBN-N domain. These findings indicate notable evolutionary differences within the *IMPβ* gene family in *TKS*, with members sharing close evolutionary relationships exhibiting similar domain compositions. For example, *TkIMPβ8* and *TkIMPβ13* in subgroup J contained the IBN-N, Xpo1, and CRM1-C domains, which facilitate the export of proteins carrying leucine-rich nuclear export signals. Based on this, we can infer the functions of *TKS IMPβ* family members by drawing comparisons with *IMPβ* homologs in Arabidopsis and other species. This insight provides a valuable foundation for further research into the functions of the IMPβ family in *TKS*.

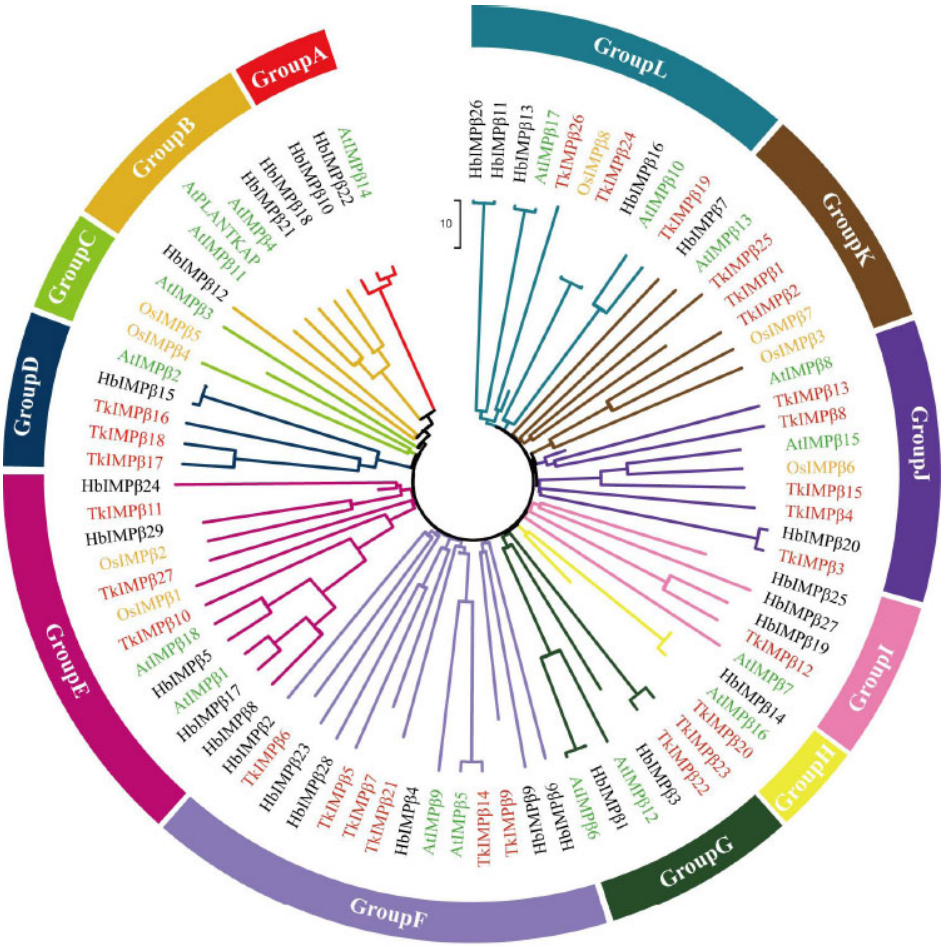

Fig. (3). Phylogenetic tree of *IMPβ* families in *TKS* and other plants. Proteins of Tk. *Taraxacum kok-saghyz*; At. *Arabidopsis thaliana*; Os. *Oryza sativa*; Hb. *Hevea brasiliensis* (in colour according to their respective classes).

3.4. Exon-intron Structure Analysis of the IMPβ Gene Family in TKS

Figure **4** illustrates the complex gene structure of the *IMPβ* family in *TKS*. Notably, TkIMPβ3, *TkIMPβ12*, and *TkIMPβ21* have a simple structure comprised of a single exon and no introns. In contrast, most TkIMPβs exhibit a more complex organization, containing over 15 exons and introns (Fig. **4**). The number of exons across all TkIMPβs ranges from 1 to 31, with closely related members displaying similar exon-intron patterns, as observed in *TkIMPβ24* and *TkIMPβ26*. The intron-exon structures of the identified paralogs—*TkIMPβ1*/*TkIMPβ2*, *TkIMPβ9*-/*TkIMPβ14*, *TkIMPβ17*/*TkIMPβ18*, and *TkIMPβ22*-/*TkIMPβ23*—were nearly identical. Protein motif and amino acid length analyses further highlight the functional diversification of the 27 *TkIMPβ* family members. These findings suggest that *TkIMPβ* family members may have diverse roles in nuclear-cytoplasmic transport.

3.5. Distribution of Cis-acting Elements in the Promoter Regions of the IMPβ Gene Family in TKS

The upstream nucleic acid sequences (2000 bp) preceding the transcription start sites of *IMPβ* genes were obtained to examine the distribution of cis-acting elements in the promoter regions. The results were organized according to the phylogenetic tree sequence and represented using different colors or shapes in Fig. (**5**). By integrating these findings with the statistics in Table **3**, it was possible to demonstrate that the promoter regions of *TkIMPβ* genes contain various cis-acting elements. Specifically, these include three elements related to transcription initiation, five associated with growth, 11 linked to hormone responses, four involved in stress responses, and 18 responsive to light. These findings suggest that the expression of *TkIMPβ* genes is regulated by different stress factors and hormones. Notably, the promoter regions of *TkIMPβ17* and *TkIMPβ18*, which are involved in replication, exhibit similar distributions of cis-acting elements.

Table 3. Information regarding cis-acting elements in the promoter regions of *TkIMPβ* genes.

Element Properties	Name
Transcription initiation-related cis-elements	CAAT-box, TATA-box, AT-rich sequence
Growth-related cis-elements	ARE, circadian, CAT-box, GCN4_motif, HD-Zip1
Hormone responsive cis-elements	TGA-element, TATC-box, TCA-element, SARE, ABRE, AuxRR-core, TGACG-motif, CGTCA-motif, P-box, GARE-motif, TGA-box
Stress response-related cis-elements	TC-rich repeats, LTR, GC-motif, WUN-motif
The optical response-related cis-elements	ACE, G-Box, G-box, GT1-motif, Sp1, 3-AF1binding site, GATA-motif, TCT-motif, I-box, LAMP-element, BoxII, Gap-box, TCCC-motif, rbcS-CMA7c, chs-CMA1a, GA-motif, GATT-motif, chs-CMA2a

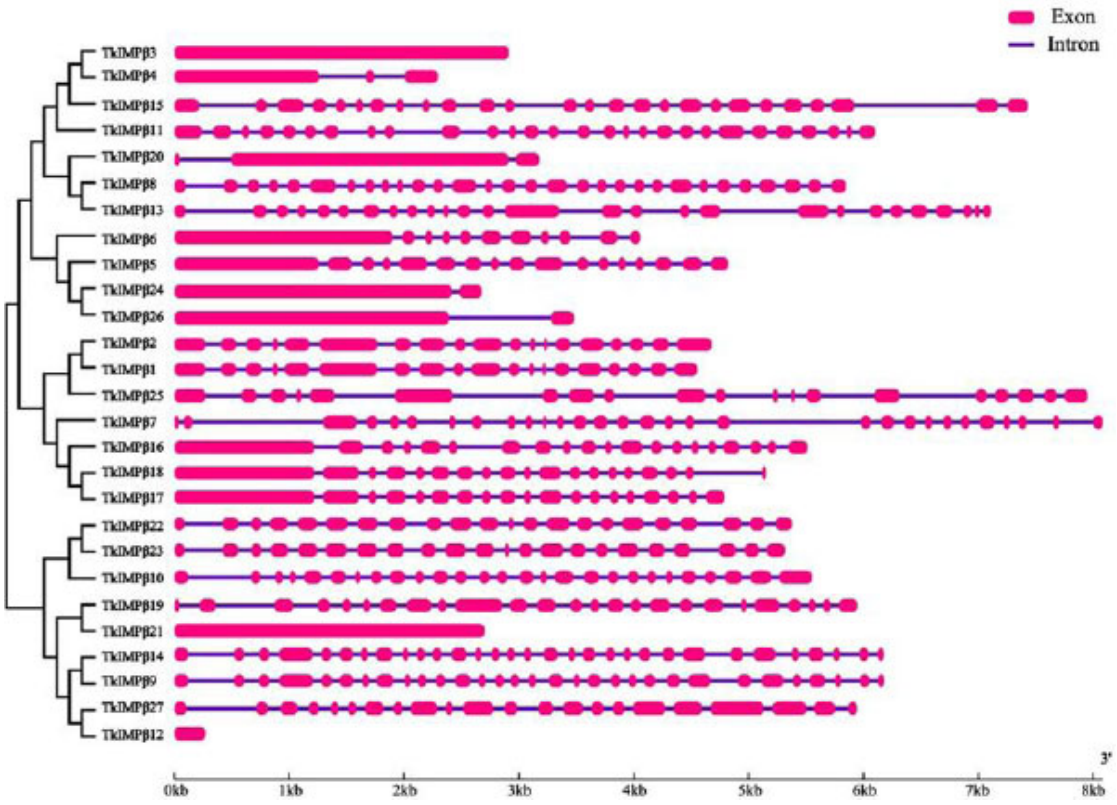

Fig. (4). Phylogenetic relationships, domain composition, and intron-exon structures of *TKS* HMTs and HDMs.

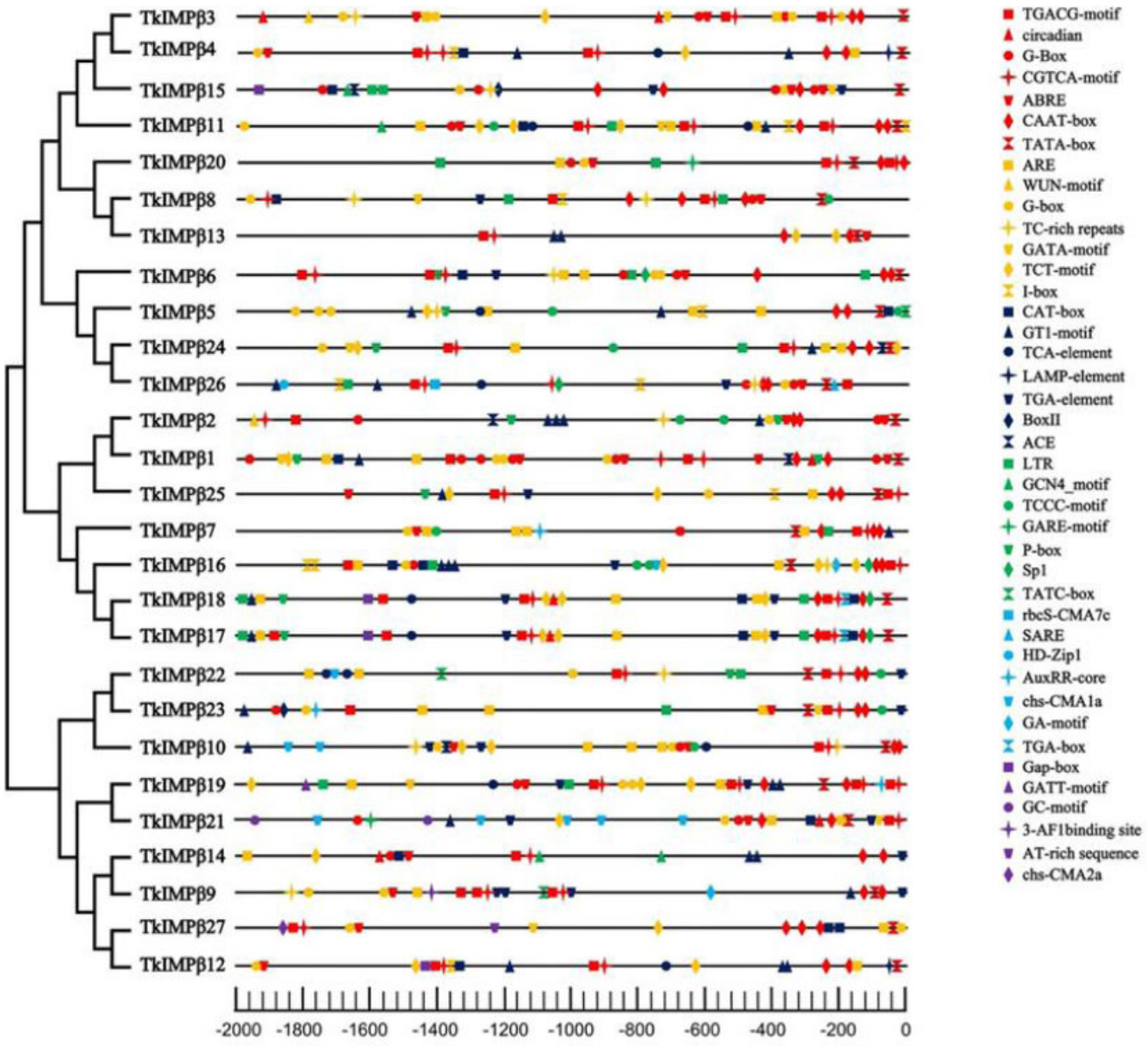

Fig. (5). Distribution of cis-elements in the promoter regions of *TkIMPβ* genes.

3.6. Expression Pattern Analysis of IMPβ Gene Family Members in TKS

To further assess the functions of *IMPβ* gene family members in *TKS* and their role in regulating the synthesis of natural rubber biosynthetic proteins, transcriptome data were used to analyze the expression profiles of 27 *TkIMPβ* genes. Root and mature leaf samples were selected for this analysis at growth stages of 1, 2, 6, 12, and 18 months (M). Expression analysis of the 27 *TkIMPβ* genes revealed that *TkIMPβ3*, *TkIMPβ5*, *TkIMPβ7*, *TkIMPβ13*, *TkIMPβ16*, *TkIMPβ23*, and *TkIMPβ24* maintained stable expression in both roots and leaves, suggesting that these genes may have essential functions in these tissues, particularly in nuclear transport. In contrast, *TkIMPβ1*, *TkIMPβ2*, *TkIMPβ4*, *TkIMPβ12*, *TkIMPβ14*, and *TkIMPβ21* exhibited lower expression levels, indicating that their roles may be less significant under normal growth conditions.

In the roots from 2M to 6M, except for *TkIMPβ10*, *TkIMPβ15*, *TkIMPβ19*, and *TkIMPβ26*, the expression levels of other genes remained largely unchanged. The expression levels of TkIMPβ19 initially decreased and then increased, whereas those of *TkIMPβ10*, *TkIMPβ15*, and *TkIMPβ26* exhibited the opposite trend. Compared with 6-month-old roots, only the expression levels of *TkIMPβ3*, *TkIMPβ4*, *TkIMPβ5*, *TkIMPβ12*, *TkIMPβ16*, *TkIMPβ20*, *TkIMPβ21*, and *TkIMPβ24* remained relatively stable in 12-month-old roots, while the remaining genes showed a

decreasing trend. Compared with 12-month-old roots, *TkIMPβ3*, *TkIMPβ5*, *TkIMPβ16*, and *TkIMPβ25* maintained high expression levels in 18-month-old roots, whereas *TkIMPβ20* showed a decline. The expression levels of all other genes increased.

Furthermore, (Fig. **6**) illustrates the growth stage-dependent peak expression levels of the 27 *TkIMPβ* genes in roots. Analysis of genes expressed at high and moderate levels showed that *TkIMPβ13*, *TkIMPβ23*, and *TkIMPβ24* exhibited the highest expression at the 1M stage, while *TkIMPβ3*, *TkIMPβ5*, *TkIMPβ7*, and *TkIMPβ16* peaked at the 18 M stage. The remaining genes had their highest expression at either the 2M or 6M stages. Thus, the expression levels of *TkIMPβ1*, *TkIMPβ2*, *TkIMPβ4*, *TkIMPβ12*, *TkIMPβ14*, and *TkIMPβ21* peaked at specific stages of root development but remained consistent throughout growth and development.

Within the *TkIMPβ* family of 27 members, *TkIMPβ3*, *TkIMPβ5*, *TkIMPβ7*, *TkIMPβ13*, *TkIMPβ16*, *TkIMPβ23*, and *TkIMPβ24* exhibited high expression levels in mature *TKS* leaves, with *TkIMPβ16* showing the highest expression. In contrast, the remaining members displayed minimal, barely detectable expression. A comparative analysis of expression levels between roots and mature leaves at 18 M revealed significant differences in *TkIMPβ10*, *TkIMPβ19*, *TkIMPβ20*, *TkIMPβ22*, *TkIMPβ25*, and *TkIMPβ27*, indicating that these genes are primarily expressed in roots rather than leaves.

3.7. Subcellular Localization

To explore the potential functions of *TkIMPβ10*, *TkIMPβ11*, and *TkIMPβ27*, we performed subcellular localization studies by injecting Agrobacterium cultures containing 35S::GFP-*TkIMPβ10*, 35S::GFP-*TkIMPβ11*, and 35S::GFP-*TkIMPβ27* vectors into *Nicotiana benthamiana* leaves. As shown in Fig. (**7**), the GFP fluorescence signal mainly appeared in the nucleus. Compared with the 35S::GFP empty vector control, fluorescence signals of 35S::GFP- *TkIMPβ10*, 35S::GFP- *TkIMPβ11*, and 35S::GFP-*TkIMPβ27* were also detected in the nucleus.

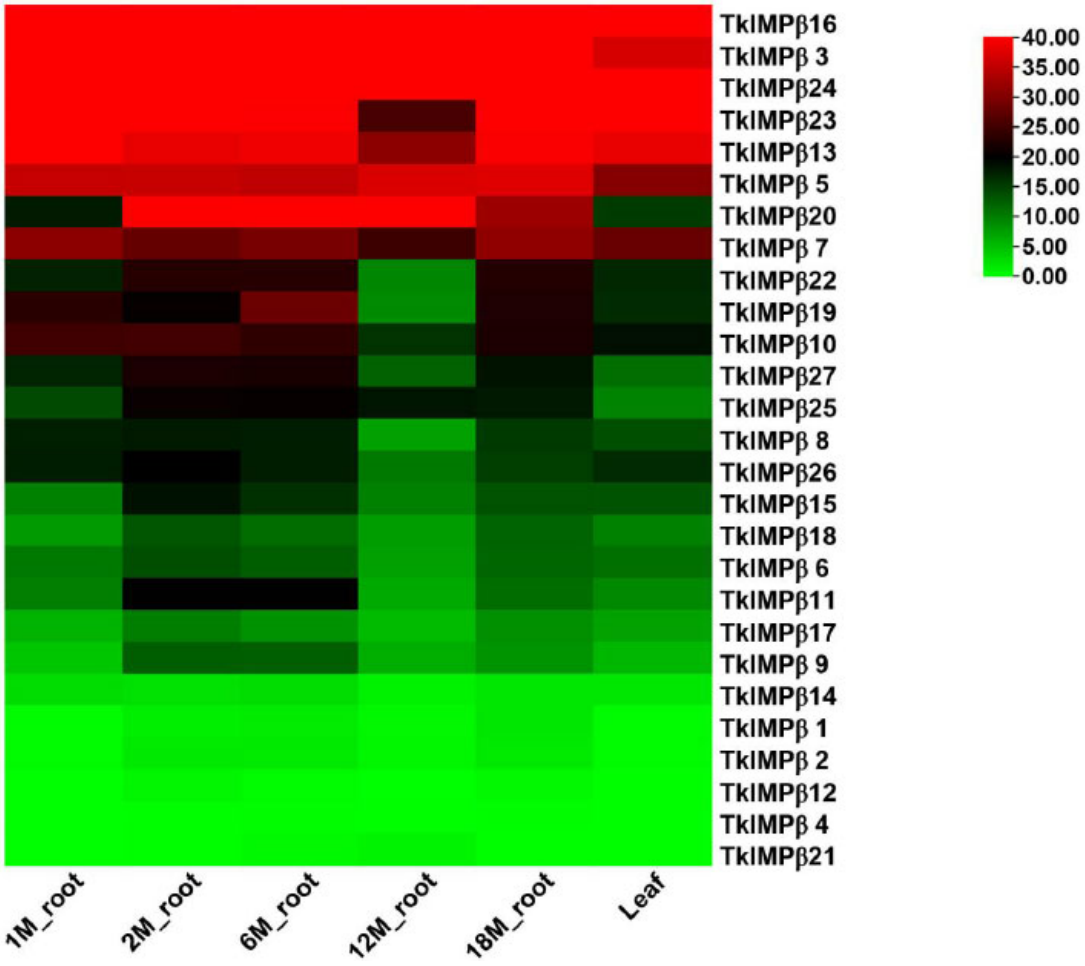

Fig. (6). Expression profiles of *TkIMPβ* genes with hierarchical clustering in roots and mature leaves from 1M to 18M. The heatmap color scale on the right indicates expression levels: red represents high transcript abundance, and green represents low transcript abundance.

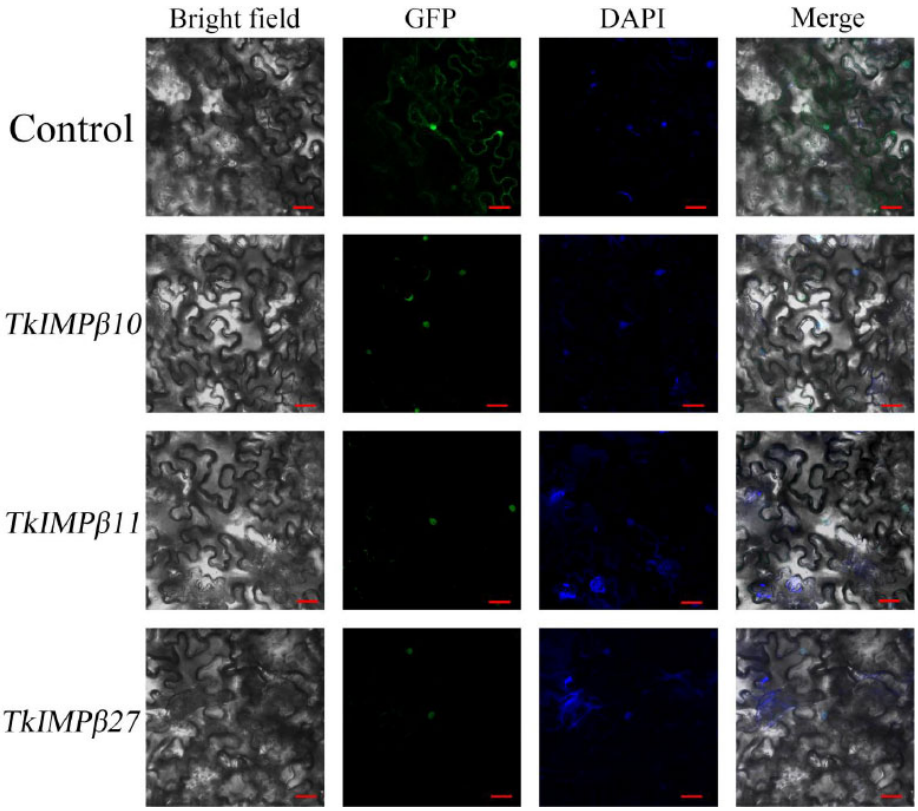

Fig. (7). Subcellular localization of *TkIMPβ10*, *TkIMPβ11*, and *TkIMPβ27*. *Nicotiana benthamiana* leaves transformed with 35S::GFP served as controls. Green represents the fluorescent signal of green fluorescent protein (GFP), blue indicates the nucleus visualized by DAPI staining, and "Merge" shows the merged images.

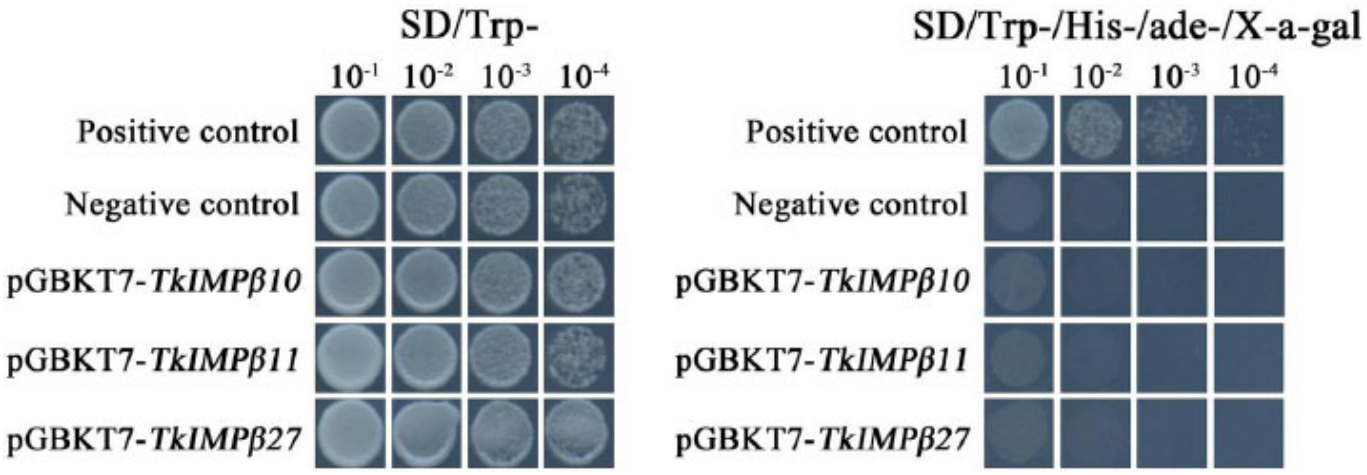

Fig. (8). Transcriptional activity analysis of *TkIMPβ10*, *TkIMPβ11*, and *TkIMPβ27*. Ad-SV40 large T-antigen was used as a positive control, and the pGBKT7 empty vector served as a negative control.

3.8. Yeast Two-hybrid Transcriptional Activation Analysis

In this study, the Y2HGold-GAL4 system was used to test whether *TkIMPβ10*, *TkIMPβ11*, and *TkIMPβ27* exhibit autoactivating transcriptional activity, with the empty pGBKT7 vector as a negative control. BD-p53 and AD-SV40 large T antigen served as positive controls (Fig. **8**). All transformed yeast cells grew normally on SD/Trp

medium. However, on SD/Trp-/His-/Ade- medium, only the positive control showed normal growth, while the negative control and yeast cells transformed with *TkIMPβ10*, *TkIMPβ11*, and *TkIMPβ27* recombinant vectors failed to grow. This indicates that *TkIMPβ10*, *TkIMPβ11*, and *TkIMPβ27* lack transcriptional activity in yeast cells.

3.9. The Expression Levels of TkIMPβ10, TkIMPβ11 and TkIMPβ27 Genes After NaCl and Hormone Treatment

In this study, we analyzed the mRNA expression levels of *TkIMPβ10*, *TkIMPβ11*, and *TkIMPβ27* in *TKS* under NaCl salt stress and methyl jasmonate (MeJA) and ethylene (Eth) treatments for 6, 12, and 24 h. As shown in Fig. (**9A**), *TkIMPβ10* expression remained unchanged after 6 and 12 hours of MeJA treatment compared with the control (CK). However, *TkIMPβ11* and *TkIMPβ27* were significantly downregulated at 6 h ($p < 0.05$, LSD test). By 24 hours, all three genes showed their lowest expression levels ($p < 0.05$, LSD test). In Fig. (**9B**), under Eth treatment, the expression of *TkIMPβ10*, *TkIMPβ11*, and *TkIMPβ27* significantly decreased at 6 and 12 h compared with CK but rebounded by 24 h. In Fig. (**9C**), under NaCl stress, none of the genes showed significant expression changes at 6 hours. However, their expression levels significantly decreased at 12 h. By 24 h, expression partially recovered but remained significantly lower than CK ($p < 0.05$, LSD test).

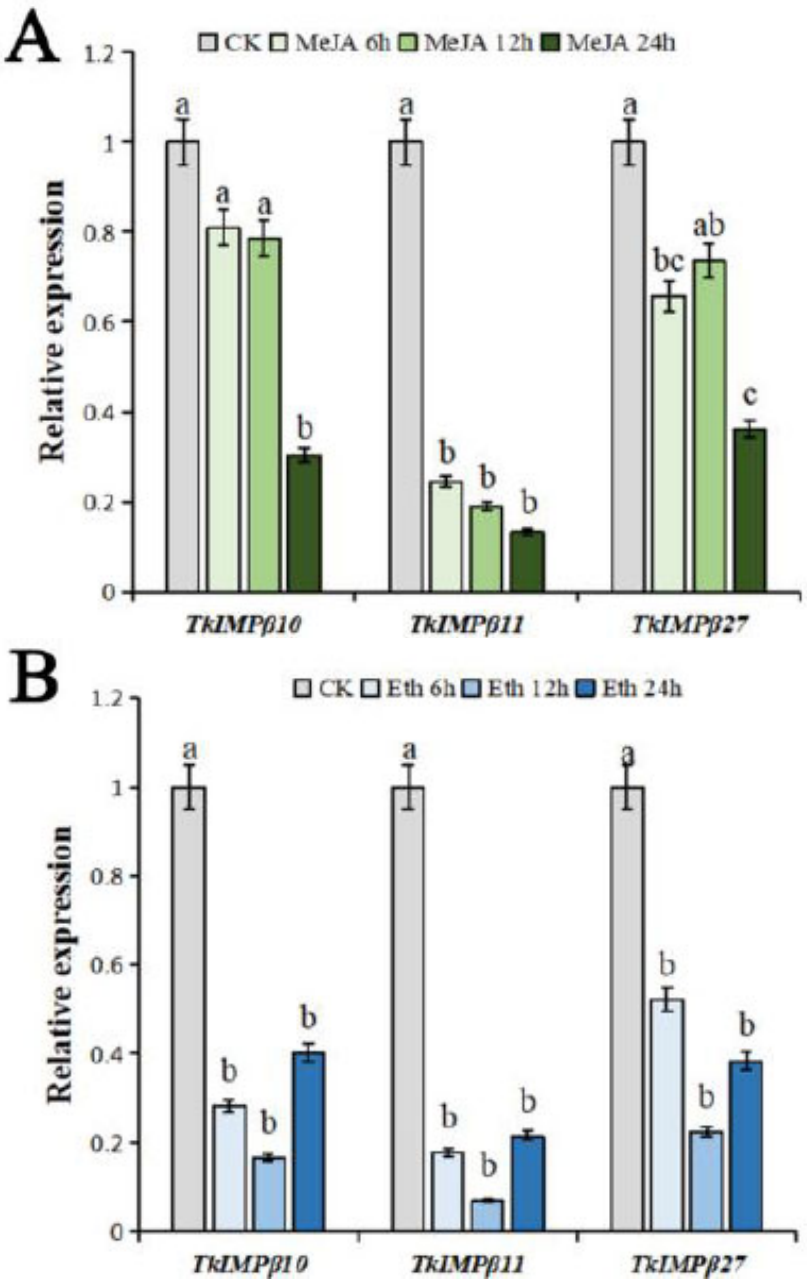

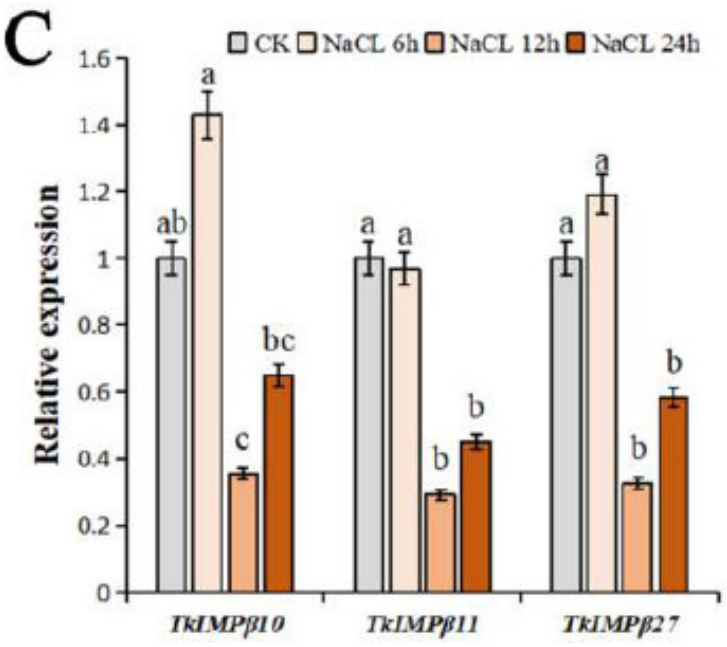

Fig. (9). The expression levels of *TkIMPβ10*, *TkIMPβ11*, and *TkIMPβ27* in *TKS* under NaCl stress and treatment with methyl jasmonate (MeJA) and ethylene (Eth) for 6, 12, and 24 hours. (**A**) Expression changes of *TkIMPβ10*, *TkIMPβ11*, and *TkIMPβ27* in response to MeJA treatment. (**B**) Expression changes of *TkIMPβ10*, *TkIMPβ11*, and *TkIMPβ27* in response to Eth treatment. (**C**) Expression changes of *TkIMPβ10*, *TkIMPβ11*, and *TkIMPβ27* under NaCl stress. The error bar represents the mean ± standard error (Mean ± SE) of the three biological replicates. Different letters indicate significant differences ($p < 0.05$, LSD).

4. DISCUSSION

The organization of life-sustaining processes and the precise regulation of cellular functions depend on the controlled movement of biological macromolecules between the nucleus and cytoplasm [39]. Disruptions in the nuclear transport regulation can lead to substrate transport irregularities, potentially contributing to disease development and progression. In eukaryotic cells, DNA transcription occurs in the nucleus, while protein synthesis takes place in the cytoplasm. The nuclear membrane serves as a barrier, separating these compartments [40], making the transport of molecules across it essential for cell function [41]. While ions, metabolites, and some small neutral proteins diffuse passively, molecules larger than 40 kDa require active transport mechanisms, utilizing transport factors within the nuclear pore complex for import and export [42]. In plant cells, this selective bidirectional transport regulates diverse cellular activities, maintains physiological balance, controls differentiation, and enables responses to environmental signals and stress through processes like signal transduction and gene expression [43].

Importin-β (IMPβ) family members are nuclear transporters widely distributed in eukaryotes. They function as nuclear transport receptors, forming complexes with cargo in the cytoplasm (where RanGTP levels are low) and releasing them in the nucleus upon RanGTP binding [44]. Typically weighing 95–145 kDa with low sequence similarity, IMPβ members share a conserved structure: an N-terminal Ran-binding domain, a central HEAT repeat domain, and a C-terminal domain for substrate or adaptor protein binding [45]. In plants, the IMPβ family regulates crucial processes such as hormone signaling, flowering, pathogen resistance, and stress tolerance [20]. This study identified 27 members of the *TkIMPβ* gene family in *TKS*. Chromosome location indicated that most are nuclear-localized.

Evolutionary analysis across *Arabidopsis thaliana*, *Hevea brasiliensis*, *Oryza sativa*, and *TKS* classified the IMPβ genes into 12 distinct families based on sequence conservation. The expansion to 27 members in *TKS*, compared to approximately 17 in *Arabidopsis* but similar to 27 in *Zea* [20], suggests a complex and potentially specialized nuclear transport network in *TKS*. This expansion may underpin its need to integrate precise developmental and environmental signals, particularly those related to rubber biosynthesis and adaptation to temperate climates. Notably, homologs such as AtIMPβ1 /*AtKPNB1* in *Arabidopsis* are positive regulators of growth, and Os*IMPβ1* in *Oryza sativa* is pollen-specific [46]. The identification of *TKS* homologs within these conserved subfamilies allows for functional predictions. For instance, *TkIMPβ10*, *TkIMPβ11*, and *TkIMPβ27* cluster in the same phylogenetic subgroup (E) as *OsIMPβ1*, *OsIMPβ2*, and *AtIMPβ1*, suggesting conserved roles in growth and development.

Gene structure analysis revealed that while *TkIMPβ3*, *TkIMPβ12*, and *TkIMPβ21* are intronless, most members

contain over 15 introns and exons. Duplicated gene pairs *TkIMPβ1/TkIMPβ2*, *TkIMPβ9/TkIMPβ14*, *TkIMPβ17-/TKIMPβ18*, and *TkIMPβ22/TkIMPβ23* exhibit nearly identical intron-exon structures, a pattern often linked to tandem duplication and the emergence of new genes with specialized functions[47]. Motif analysis further supports functional diversification. The conserved motifs enriched in HEAT and IBN-N domains form the superhelical skeleton essential for interactions with the NPC, RanGTPase, and cargo proteins [36, 37]. The distinct motif composition between importins (*e.g.*, IBN-N-containing) and exportins (*e.g.*, Xpo1-containing) underlies their transport direction specificity. Member-specific motifs, such as Motif 31 in *TkIMPβ7*, likely reside in variable loop regions critical for substrate recognition [38, 39], potentially enabling the transport of unique cargoes, including transcription factors specific to rubber biosynthesis or stress responses.

Expression analysis revealed distinct patterns among *TkIMPβ* members. *TkIMPβ10*, *TkIMPβ19*, *TkIMPβ20*, and *TkIMPβ22* were preferentially expressed in roots, the primary site of natural rubber biosynthesis (NRB) in TKS, implying a critical role in this process. In contrast, *TkIMPβ1*, *TkIMPβ2*, *TkIMPβ4*, *TkIMPβ12*, *TkIMPβ14*, and *TkIMPβ21* remained largely unchanged, indicating their potential function as housekeeping genes, which requires more in-depth investigation. Our findings collectively demonstrate the essential role of TkIMPβ family members in natural rubber production and suggest that these genes could serve as valuable resources for investigating rapid changes in NRB-related protein content following exposure to heavy metals in future studies. Recently, a total of 102 NRB-related gene and protein members were identified, including 10 cis-isoprene transferases (CPT), 8 small rubber particle proteins (SRPP), 2 rubber elongation factors (REF), and one HRT1-REF bridging protein (HRBP). Among these, CPT7, SRPP5, SRPP6, and SRPP9 might play more important roles in NRB within *TKS* roots [35]. Given this, it would be valuable to prioritize research on the relationships between IMPβ gene family members and genes and proteins involved in natural rubber biosynthesis (NRB).

Based on the phylogenetic tree and expression patterns of IMPβ gene family members in *TKS*, we selected *TkIMPβ10*, *TkIMPβ11*, and *TkIMPβ27* for subcellular localization analysis. In the phylogenetic tree, these genes belong to the E subgroup, where their *Arabidopsis* and rubber tree counterparts are associated with growth and development. Therefore, we speculate that *TkIMPβ10*, *TkIMPβ11*, and *TkIMPβ27* belong to the same subfamily as *OsIMPβ1*, *OsIMPβ2*, and *AtIMPβ1* and may have similar functions. Subcellular localization analysis revealed that *TkIMPβ10*, *TkIMPβ11*, and *TkIMPβ27* were primarily expressed in the nucleus, suggesting their potential roles in nuclear material transport or signal transduction. Additionally, latex cell development is the most active before 6M. The expression patterns of these genes in *TKS* showed peak expression in roots at 2M and 6M, followed by a significant decline at 12M, with little to no expression in leaves. Further yeast two-hybrid assays confirmed that they lack intrinsic transcriptional activation, indicating that they function not as transcription factors but likely as transporters facilitating the nuclear import of cargo proteins. This aligns with the canonical role of IMPβ family members.

To further investigate the specific roles of *TkIMPβ10*, *TkIMPβ11*, and *TkIMPβ27* in rubber biosynthesis and plant responses to environmental stress, we conducted NaCl stress and MeJA and Eth hormone treatments. In the NaCl stress experiment, the expression of these genes decreased at 12 h but increased by 24 hours, a biphasic response common in stress-adaptive genes [48, 49].

In the MeJA treatment experiment, *TkIMPβ11* and *TkIMPβ27* showed a rapid downregulation at 6h, indicating a role in the early MeJA response. *TkIMPβ10* responded later, suggesting differential regulation within the family for fine-tuning JA-mediated processes, which are central to induced defense and rubber biosynthesis [50]. In the Eth treatment experiment, the expression levels of *TkIMPβ10*, *TkIMPβ11*, and *TkIMPβ27* significantly decreased after 6 and 12 h of treatment but increased after 24 h. These findings suggest that these genes may be involved in ethylene signal transduction. Previous studies reported a similar response in *Synechocystis*, where Eth treatment caused a rapid but transient decrease in transcript levels of etr1, slr1213, and slr1214 during phototaxis [51]. Hence, we conclude that a comprehensive analysis of the IMPβ family in additional rubber-producing plants, such as *Parthenium hysterophorus* and *Eucommia ulmoides*, could provide deeper insights into the role of IMPβ genes in regulating natural rubber biosynthesis.

Notably, three nuclear localization genes—*TkIMPβ10*, *TkIMPβ11*, and *TkIMPβ27* (Fig. **7**)—are preferentially expressed during development but show a significant negative correlation under salt stress, MeJA, and Eth treatments. Similarly, previous research has demonstrated that cis-acting elements play a crucial role in plant responses to abiotic stress as well as growth and development [52, 53]. Our analysis of *TkIMPβ* cis-elements revealed numerous stress- and hormone-responsive cis-elements in the promoter regions of *TkIMPβ10*, *TkIMPβ11*, and *TkIMPβ27* (Fig. **5**). For example, all three contain MeJA response elements (TGACG-motif, CGTCA-motif) and the abiotic stress response element ABRE, which are key regulators of plant defense against biotic and abiotic stresses. Additionally, most TkIMPβ members contain Tc-rich repeats and MBS [54], which are essential for plant stress response and defense. These findings align with previous research, indicating that SAPs are closely associated with stress responses [55].

CONCLUSION

In conclusion, the analysis of the IMPβ gene family in *TKS* provides valuable insights into its functions and regulatory mechanisms. Genomic data acquisition and subsequent analysis identified 27 TkIMPβ family members, a number comparable to that in other plant species. Gene

structure analysis revealed both similarities and variations among members with replication-based relationships, indicating evolutionary differentiation. Phylogenetic analysis classified the TkIMPβ family into subfamilies and identified four groups of replication factors. Additionally, expression analysis indicated that some *TkIMPβ* genes are closely linked to rubber production-related functions, suggesting their role in regulating natural rubber synthesis. Subcellular localization and yeast two-hybrid experiments confirmed that *TkIMPβ10*, *TkIMPβ11*, and *TkIMPβ27* are not transcription factors but function as nuclear transport proteins involved in the transport or signal transduction of nuclear substances. Further experiments involving NaCl stress and MeJA and Eth hormone treatments explored the specific roles of *TkIMPβ10*, *TkIMPβ11*, and *TkIMPβ27* in rubber biosynthesis and plant responses to environmental stress. These findings provide a comprehensive understanding of the evolution and expression patterns of the IMPβ family in *TKS* and offer potential gene targets for molecular breeding strategies aimed at enhancing rubber production. Overall, this study expands our knowledge of the IMPβ gene family in *TKS*, paving the way for further research and practical applications in the field.

AUTHORS' CONTRIBUTIONS

The authors confirm contribution to the paper as follows: Q.Y. and W.M.: Contributed to the study conception and design, and data acquisition; W.M. and X.Z..: Performed the data analysis; Q.Y. and W.M.: The first draft of the manuscript was written by, and all authors commented on previous versions. X.Z.: Critically reviewed and edited the manuscript with supervision. All authors read and approved the final manuscript.

LIST OF ABBREVIATIONS

TKS	=	Taraxacum Kok-Saghyz
IMPβ	=	Importin Β
TkIMPβ	=	TKS importin β
MeJA	=	Methyl Jasmonate
NR	=	Natural Rubber
CAS	=	Cellular Apoptosis Susceptibility

ETHIC APPROVAL AND CONSENT TO PARTICIPATE

Not applicable.

HUMAN AND ANIMAL RIGHTS

Not applicable.

CONSENT FOR PUBLICATION

Not applicable.

AVAILABILITY OF DATA AND MATERIALS

All data generated or analyzed during this study are included in this published article.

FUNDING

None.

CONFLICT OF INTEREST

The authors declare no conflict of interest, financial or otherwise.

ACKNOWLEDGEMENTS

We particularly thank Dr. Lingling Wang and Dr. Qi Yao from Hainan Normal University for their generous support.

REFERENCES

[1] Men X, Wang F, Chen GQ, Zhang HB, Xian M. Biosynthesis of natural rubber: current state and perspectives. Int J Mol Sci 2018; 20(1): 50. http://dx.doi.org/10.3390/ijms20010050 PMID: 30583567

[2] Warren-Thomas E, Dolman PM, Edwards DP. Increasing demand for natural rubber necessitates a robust sustainability initiative to mitigate impacts on tropical biodiversity. Conserv Lett 2015; 8(4): 230-41. http://dx.doi.org/10.1111/conl.12170

[3] Xie Q, Ding G, Zhu L, *et al*. Proteomic landscape of the mature roots in a rubber-producing grass *Taraxacum kok-saghyz*. Int J Mol Sci 2019; 20(10): 2596. http://dx.doi.org/10.3390/ijms20102596 PMID: 31137823

[4] Luo Z, Iaffaldano BJ, Zhuang X, Fresnedo-Ramírez J, Cornish K. Analysis of the first *Taraxacum kok-saghyz* transcriptome reveals potential rubber yield related SNPs. Sci Rep 2017; 7(1): 9939. http://dx.doi.org/10.1038/s41598-017-09034-2 PMID: 28855528

[5] Salehi M, Cornish K, Bahmankar M, Naghavi MR. Natural rubber-producing sources, systems, and perspectives for breeding and biotechnology studies of *Taraxacum kok-saghyz*. Ind Crops Prod 2021; 170: 113667. http://dx.doi.org/10.1016/j.indcrop.2021.113667

[6] Cherian S, Ryu SB, Cornish K. Natural rubber biosynthesis in plants, the rubber transferase complex, and metabolic engineering progress and prospects. Plant Biotechnol J 2019; 17(11): 2041-61. http://dx.doi.org/10.1111/pbi.13181 PMID: 31150158

[7] Amerik AY, Martirosyan L, Martirosyan VV, *et al*. Parthenium argentatum A. Gray, *Taraxacum kok-saghyz* L.E. Rodin, and *Scorzonera tau-saghyz* Lipsch. et Bosse as alternative sources of natural rubber: do we really need them? Sh Biol 2022; 57(1): 3-26. http://dx.doi.org/10.15389/agrobiology.2022.1.3eng

[8] Chen J, Wang W, Dong Y, *et al*. Optimization of extraction of inulin from Taraxacum kok-saghyz Rodin by response surface methodology and its MALDI-TOF MS analysis. Sci Technol Food Ind 2022; 43(1): 205-12. http://dx.doi.org/10.13386/j.issn1002-0306.2021040173

[9] Tempel S, Bedo J, Talla E. From a large-scale genomic analysis of insertion sequences to insights into their regulatory roles in prokaryotes. BMC Genomics 2022; 23(1): 451. http://dx.doi.org/10.1186/s12864-022-08678-3 PMID: 35725380

[10] Pavithra Bhavanasi , Bhavanasi P, Bollapragada RS. Understanding cell biology. International J Res Phytochem Pharmacol Sci 2019; 1(1): 39-45. http://dx.doi.org/10.33974/ijrpps.v1i1.108

[11] Pemberton LF, Paschal BM. Mechanisms of receptor-mediated nuclear import and nuclear export. Traffic 2005; 6(3): 187-98. http://dx.doi.org/10.1111/j.1600-0854.2005.00270.x PMID: 15702987

[12] Raices M, D'Angelo MA. Structure, maintenance, and regulation of nuclear pore complexes: The gatekeepers of the eukaryotic genome. Cold Spring Harb Perspect Biol 2022; 14(3): a040691. http://dx.doi.org/10.1101/cshperspect.a040691 PMID: 34312247

[13] Chook Y, Blobel G. Karyopherins and nuclear import. Curr Opin Struct Biol 2001; 11(6): 703-15. http://dx.doi.org/10.1016/S0959-440X(01)00264-0 PMID: 11751052

[14] Conti E, Müller CW, Stewart M. Karyopherin flexibility in nucleocytoplasmic transport. Curr Opin Struct Biol 2006; 16(2): 237-44.
http://dx.doi.org/10.1016/j.sbi.2006.03.010 PMID: 16567089

[15] Sumner MC, Brickner J. The nuclear pore complex as a transcription regulator. Cold Spring Harb Perspect Biol 2022; 14(1): a039438.
http://dx.doi.org/10.1101/cshperspect.a039438 PMID: 34127448

[16] Fahrenkrog B, Aebi U. The nuclear pore complex: nucleocytoplasmic transport and beyond. Nat Rev Mol Cell Biol 2003; 4(10): 757-66.
http://dx.doi.org/10.1038/nrm1230 PMID: 14570049

[17] Macara IG. Transport into and out of the Nucleus. Microbiol Mol Biol Rev 2001; 65(4): 570-94.
http://dx.doi.org/10.1128/MMBR.65.4.570-594.2001 PMID: 11729264

[18] Fried H, Kutay U. Nucleocytoplasmic transport: Taking an inventory. Cell Mol Life Sci 2003; 60(8): 1659-88.
http://dx.doi.org/10.1007/s00018-003-3070-3 PMID: 14504656

[19] Petrovic S, Mobbs GW, Bley CJ, Nie S, Patke A, Hoelz A. Structure and function of the nuclear pore complex. Cold Spring Harb Perspect Biol 2022; 14(12): a041264.
http://dx.doi.org/10.1101/cshperspect.a041264 PMID: 36096637

[20] Jin L, Zhang G, Yang G, Dong J. Identification of the Karyopherin Superfamily in Maize and Its Functional Cues in Plant Development. Int J Mol Sci 2022; 23(22): 14103.
http://dx.doi.org/10.3390/ijms232214103 PMID: 36430578

[21] Xu Y, Liu L, Zhao P, *et al*. Genome-Wide Identification, Expression Profile and Evolution Analysis of Karyopherin β Gene Family in *Solanum tuberosum* Group Phureja DM1-3 Reveals Its Roles in Abiotic Stresses. Int J Mol Sci 2020; 21(3): 931.
http://dx.doi.org/10.3390/ijms21030931 PMID: 32023817

[22] Liu L, Liu Y, Ji X, Zhao X, Liu J, Xu N. Coronatine orchestrates ABI1 -mediated stomatal opening to facilitate bacterial pathogen infection through importin β protein SAD2. Plant J 2024; 119(2): 676-88.
http://dx.doi.org/10.1111/tpj.16784 PMID: 38683723

[23] Li Q, Zheng J, Li S, *et al*. Transporter-mediated nuclear entry of jasmonoyl-isoleucine is essential for jasmonate signaling. Mol Plant 2017; 10(5): 695-708.
http://dx.doi.org/10.1016/j.molp.2017.01.010 PMID: 28179150

[24] Artimo P, Jonnalagedda M, Arnold K, *et al*. ExPASy: SIB bioinformatics resource portal. Nucleic Acids Res 2012; 40(W1): W597-603.
http://dx.doi.org/10.1093/nar/gks400 PMID: 22661580

[25] Tang K, Dong CJ, Liu JY. Genome-wide comparative analysis of the phospholipase D gene families among allotetraploid cotton and its diploid progenitors. PLoS One 2016; 11(5): e0156281.
http://dx.doi.org/10.1371/journal.pone.0156281 PMID: 27213891

[26] Yu K, Zhao Z, Gao A, *et al*. Cloning and expression analysis of phytoene desaturase (PDS) gene from mango (*Mangifera indica* L). Computational Molecular Biology 2022; 12(4): 1-8.
http://dx.doi.org/10.5376/cmb.2022.12.0004

[27] Bailey TL, Williams N, Misleh C, Li WW. MEME: discovering and analyzing DNA and protein sequence motifs. Nucleic Acids Res 2006; 34(Web Server): W369-73.
http://dx.doi.org/10.1093/nar/gkl198 PMID: 16845028

[28] Tamura K, Stecher G, Peterson D, Filipski A, Kumar S. MEGA6: Molecular evolutionary genetics analysis version 6.0. Mol Biol Evol 2013; 30(12): 2725-9.
http://dx.doi.org/10.1093/molbev/mst197 PMID: 24132122

[29] Hu B, Jin J, Guo AY, Zhang H, Luo J, Gao G. GSDS 2.0: An upgraded gene feature visualization server. Bioinformatics 2015; 31(8): 1296-7.
http://dx.doi.org/10.1093/bioinformatics/btu817 PMID: 25504850

[30] Lescot M, Déhais P, Thijs G, *et al*. PlantCARE, a database of plant cis-acting regulatory nlms and a portal to tools for in silico analysis of promoter sequences. Nucleic Acids Res 2002; 30(1): 325-7.
http://dx.doi.org/10.1093/nar/30.1.325 PMID: 11752327

[31] Xie Q, Ma J, Ding G, *et al*. Transcriptomics and proteomics profiles of *Taraxacum kok-saghyz* roots revealed different gene and protein members play different roles for natural rubber biosynthesis. Ind Crops Prod 2022; 181: 114776.
http://dx.doi.org/10.1016/j.indcrop.2022.114776

[32] Jin X, Zhu L, Yao Q, *et al*. Expression profiling of mitogen-activated protein kinase genes reveals their evolutionary and functional diversity in different rubber tree (*Hevea brasiliensis*) cultivars. Genes (Basel) 2017; 8(10): 261.
http://dx.doi.org/10.3390/genes8100261 PMID: 28984837

[33] Yang L, Ji W, Zhu Y, *et al*. GsCBRLK, a calcium/calmodulin-binding receptor-like kinase, is a positive regulator of plant tolerance to salt and ABA stress. J Exp Bot 2010; 61(9): 2519-33.
http://dx.doi.org/10.1093/jxb/erq084 PMID: 20400529

[34] Qin B, Pan M, Yu HY, *et al*. Evaluation of reference genes for quantitative real-time PCR expression studies in *Taraxacum kok-saghyz* Rodin. Plant Physiol 2016; 52(07): 1059-65.
http://dx.doi.org/10.13592/j.cnki.ppj.2016.0170

[35] Livak KJ, Schmittgen TD. Analysis of relative gene expression data using real-time quantitative PCR and the 2(-Delta Delta C(T)) Method. Methods 2001; 25(4): 402-8.
http://dx.doi.org/10.1006/meth.2001.1262 PMID: 11846609

[36] Chakrabarty B, Parekh N. DBSTRIPS : Database of structural repeats in proteins. Protein Sci 2022; 31(1): 23-36.
http://dx.doi.org/10.1002/pro.4052 PMID: 33641184

[37] Parker JB, Tenorio CA, Blaber M. The ubiquitous buried water in the BETA-TREFOIL architecture contributes to the folding nucleus and ~20% of the folding enthalpy. Protein Sci 2021; 30(11): 2287-97.
http://dx.doi.org/10.1002/pro.4192 PMID: 34562298

[38] Chen X, Cai X, Chen Z, *et al*. Mosaic evolution of beta-barrel-porin-encoding genes in *Escherichia coli*. Appl Environ Microbiol 2022; 88(7): e00060-22.
http://dx.doi.org/10.1128/aem.00060-22 PMID: 35285711

[39] Tran EJ, King MC, Corbett AH. Macromolecular transport between the nucleus and the cytoplasm: Advances in mechanism and emerging links to disease. Biochim Biophys Acta Mol Cell Res 2014; 1843(11): 2784-95.
http://dx.doi.org/10.1016/j.bbamcr.2014.08.003 PMID: 25116306

[40] Cooper GM. The nuclear envelope and traffic between the nucleus and cytoplasm structure of the nuclear envelope. The cell: A molecular approach. (2nd ed.). Sunderland, MA: Sinauer Associates 2000; pp. 305-30.

[41] Aggarwal A, Agrawal DK. Importins and exportins regulating allergic immune responses. Mediators Inflamm 2014; 2014: 1-14.
http://dx.doi.org/10.1155/2014/476357 PMID: 24733961

[42] Chang CW, Couñago RM, Williams SJ, Boden M, Kobe B. The distribution of different classes of nuclear localization signals (NLSs) in diverse organisms and the utilization of the minor NLS-binding site inplantnuclear import factor importin-α. Plant Signal Behav 2013; 8(10): e25976.
http://dx.doi.org/10.4161/psb.25976 PMID: 24270630

[43] Huang JG, Yang M, Liu P, Yang GD, Wu CA, Zheng CC. Genome-wide profiling of developmental, hormonal or environmental responsiveness of the nucleocytoplasmic transport receptors in *Arabidopsis*. Gene 2010; 451(1-2): 38-44.
http://dx.doi.org/10.1016/j.gene.2009.11.009 PMID: 19944133

[44] Lowe AR, Tang JH, Yassif J, *et al*. Importin-β modulates the permeability of the nuclear pore complex in a Ran-dependent manner. eLife 2015; 4: e04052.
http://dx.doi.org/10.7554/eLife.04052 PMID: 25748139

[45] Merkle T. Nucleo-cytoplasmic transport of proteins and RNA in plants. Plant Cell Rep 2011; 30(2): 153-76.
http://dx.doi.org/10.1007/s00299-010-0928-3 PMID: 20960203

[46] Luo Y, Wang Z, Ji H, *et al*. An A rabidopsis homolog of importin β1 is required for ABA response and drought tolerance. Plant J 2013; 75(3): 377-89.
http://dx.doi.org/10.1111/tpj.12207 PMID: 23582042

[47] Ma MY, Lan XR, Niu DK. Intron gain by tandem genomic duplication: a novel case in a potato gene encoding RNA-

dependent RNA polymerase. PeerJ 2016; 4: e2272. http://dx.doi.org/10.7717/peerj.2272 PMID: 27547574

[48] Das P, Majumder AL. Transcriptome analysis of grapevine under salinity and identification of key genes responsible for salt tolerance. Funct Integr Genomics 2019; 19(1): 61-73. http://dx.doi.org/10.1007/s10142-018-0628-6 PMID: 30046943

[49] Nagavi-alhoseiny AA, Torshabi M, Rasoulianboroujeni M, Tayebi L, Tabatabaei FS. Effect of sodium chloride on gene expression of *Streptococcus mutans* and zeta potential of demineralized dentin. J Oral Biol Craniofac Res 2019; 9(1): 1-4. http://dx.doi.org/10.1016/j.jobcr.2018.08.002 PMID: 30197855

[50] Fantini E, Daddiego L, Facella P, *et al*. MYC2 influences rubber and sesquiterpene lactones synthesis in Taraxacum species. Planta 2025; 262(1): 5. http://dx.doi.org/10.1007/s00425-025-04719-9 PMID: 40413374

[51] Lacey RF, Allen CJ, Bakshi A, Binder BM. Ethylene causes transcriptomic changes in *Synechocystis* during phototaxis. Plant Direct 2018; 2(3): e00048. http://dx.doi.org/10.1002/pld3.48 PMID: 31245714

[52] Li J, Han G, Sun C, Sui N. Research advances of MYB transcription factors in plant stress resistance and breeding. Plant Signal Behav 2019; 14(8): 1613131. http://dx.doi.org/10.1080/15592324.2019.1613131 PMID: 31084451

[53] Sheshadri SA, Nishanth MJ, Simon B. Stress-mediated *cis*-nlm transcription factor interactions interconnecting primary and specialized metabolism *in planta*. Front Plant Sci 2016; 7: 1725. http://dx.doi.org/10.3389/fpls.2016.01725 PMID: 27933071

[54] Li Z, Zhang J, Li J, Li H, Zhang G. The functional and regulatory mechanisms of the *Thellungiella salsuginea* ascorbate peroxidase 6 (TsAPX6) in response to salinity and water deficit stresses. PLoS One 2016; 11(4): e0154042. http://dx.doi.org/10.1371/journal.pone.0154042 PMID: 27097028

[55] Nakashima K, Yamaguchi-Shinozaki K. ABA signaling in stress-response and seed development. Plant Cell Rep 2013; 32(7): 959-70. http://dx.doi.org/10.1007/s00299-013-1418-1 PMID: 23535869